# Time-Resolved Spectral Investigation of Bacteriochlorophyll *a* and Its Transmetalated Derivatives [Zn]-Bacteriochlorophyll *a* and [Pd]-Bacteriochlorophyll *a*

**Christian Musewald,[†] Gerhard Hartwich,[†] Florian Pöllinger-Dammer,[†] Harald Lossau,[†] Hugo Scheer,[‡] and Maria Elisabeth Michel-Beyerle*,[†]**

*Institut für Physikalische und Theoretische Chemie, Technische Universität München, Lichtenbergstrasse 4, D-85748 Garching, Germany, and Botanisches Institut der Ludwig-Maximilians-Universität München, Menzinger Strasse 67, D-80638 München, Germany*

*Received: May 19, 1998; In Final Form: August 12, 1998*

The lowest excited singlet ($S_1$) and triplet ($T_1$) states of bacteriochlorophyll *a* (BChl) and its central metal derivatives [Zn]- and [Pd]- BChl were investigated by femtosecond time-resolved absorption and fluorescence spectroscopy. In contrast to previously reported dynamic solvation effects on the picosecond time scale for BChl, no short kinetic components were observed for BChl and [Zn]-BChl provided that photochemical transformations of the pigments caused by multiple excitation are avoided. The $S_1$ lifetimes of 2.6 ns, 2.1 ns, and 65 ps for BChl, [Zn]-BChl and [Pd]-BChl, respectively, are dominated by intersystem crossing (ISC) to the triplet state $T_1$. The respective triplet quantum yields amount to 76%, 85%, and >99%. The data support that [Pd]-BChl is a highly efficient photosensitizer for photodynamic tumor therapy.

## Introduction

Pigments of the tetrapyrrole type play a central role in photosynthesis.[1] They are responsible for the absorption of light and the transfer of excitation energy[2−7] as well as for the initial steps in transmembrane charge separation[8−10] in the reaction center of bacteria and the photosystems in plants. Apart from their key functions in photobiology, this class of pigments meets the requirements for photosensitizers in photodynamic tumor therapy (PDT).[11−18]

Recently, metal-substituted derivatives of bacteriochlorophyll *a* (BChl)[19−21] differing in their redox properties[19,22−26] have been introduced into the reaction center of *Rhodobacter sphaeroides* replacing the accessory pigments.[26−32] These modifications, in particular the ones carrying a [Ni]-BChl, provide strong support for the sequential mechanism also in native reaction centers.[10,33] Such studies on proteins containing metal-substituted BChls prompted us to investigate the photophysics of these pigments in solution focusing on the influence of the central metal ion on the excited-state dynamics.

So far, complexes of cyclic tetrapyrroles with divalent metal ions other than $Mg^{2+}$ were studied mainly in the chlorin (17,18-dihydroporphyrin) and in the porphyrin series focusing on their electrochemical and photophysical properties.[25,34−37] According to the four-orbital model of tetrapyrroles,[38] the four lowest allowed one-electron $\pi-\pi^*$ promotions ($a_{2u} \rightarrow e_{gy}$, $a_{1u} \rightarrow e_{gx}$, *y*-polarized, and $a_{1u} \rightarrow e_{gy}$, $a_{2u} \rightarrow e_{gx}$, *x*-polarized) are linearly combined, giving rise to the $B_y$, $Q_y$, $B_x$, and $Q_y$ absorption bands. They are pairwise degenerate in metalloporphyrins ($E(Q_x) = E(Q_y)$, $E(B_x) = E(B_y)$) because of their $D_{4h}$ symmetry. Compared to the chlorins (chlorophylls), bacteriochlorins (7,8,17,-18-tetrahydroporphyrins) and bacteriochlorophylls, in particular, are of potential advantage because all their four $\pi-\pi^*$ transitions are well separated.[24,39−41]

Previous picosecond absorption studies of metalloporphyrins (Zn, Pt, Pd, Ni)[42,43] revealed large differences in excited-state lifetimes depending on the energy of metal d-states[42] and specific spin−orbit coupling.[42,44] More recently, femtosecond spectroscopy on Ni porphyrins in two different coordination states revealed ultrafast photodissotiation of the axial ligands of the 6-fold-coordinated sample.[45,46]

In this paper we present a femtosecond time-resolved study of the excited states of [M]-BChl and its $13^2$-hydroxy derivatives with the central ions $Mg^{2+}$, $Zn^{2+}$, and $Pd^{2+}$ in toluene solution. Analogous measurements on [Ni]-BChl, where low lying metal-centered states are accessible during $S_1$ deactivation, will be published in a forthcoming paper. The results support the potential of metal-substituted BChl as photosensitizers in photodynamic therapy.[17,18] A picosecond, time-resolved, and nonlinear absorption study that complements this work and supports our conclusions on the excited-state dynamics of [M]-BChl has recently been conducted.[47]

## Materials and Methods

**Sample Preparation.** BChl was isolated from *R. sphaeroides* using standard methods.[48−50] Hydroxylation at position C-$13^2$ to $13^2$-OH−BChl was performed by storage of BChl in methanol for 5 days in the dark and subsequent silica gel chromatography.[49,51] Demetalation of BChl was achieved by treatment with small amounts of glacial acetic acid to yield BPhe.[52] [M]-BChl pigments were prepared by a transmetalation method described previously.[19] First the precursor Cd complexes were prepared by refluxing BPhe in dimethylformamide with anhydrous $Cd(OAc)_2$ and subsequent purification on silica gel. Addition of metal chlorides to a solution of the resulting [Cd]-BChl in acetone resulted in transmetalation to the respective Pd and Zn complexes. The samples were purified on silica gel.

Toluene solutions of the pigments were degassed (flushed with $N_2$), and the cuvettes were sealed in order to suppress photoinduced oxidation. The optical densities of the samples

* To whom correspondence should be addressed.
† Technische Universität München.
‡ Botanisches Institut der Ludwig-Maximilians-Universität München.

S1089-5647(98)02309-8 CCC: $15.00 
Published on Web 09/30/1998

were adjusted to OD = 1 at 780 nm for transient absorption and to OD = 0.1 at 780 nm for transient fluorescence measurements.

**Pump/Probe Absorption Spectroscopy.** For the time-resolved absorption measurements we used a pump/probe laser system based on a 76 MHz Ti:sapphire oscillator and a regenerative amplifier with a variable repetition rate of 10−1000 Hz; 100 Hz and 1 kHz used for this experiment lead to excitation rates of 50 and 500 Hz. The self-mode-locked oscillator (Coherent MIRA Basic) pumped by an $Ar^+$ laser (8 W, Coherent Innova 310, all lines) produces laser pulses at 780 nm with a duration of 100 fs ($sech^2$ pulse shape) and an average power of 500 mW. The pulses with a spectral width of 15 nm were stretched to 150 ps before seeding the regenerative amplifier system (BMI Alpha 1000S) pumped by an 8 W YLF laser (BMI 621D) at 528 nm. After amplification (1.8 mJ) the output was split into pump and probe beam (9:1) and was recompressed separately to 100 fs in two identical compressor units. The more intense pulse was used for excitation of the sample at 780 nm, and the weaker one was sent over a delay-line (0−1.5 ns, resolution 6.6 fs) before passing a white-light generation in a 10 mm flow cell containing ethanol. The white-light continuum was sent through a chirp-compensated stepper-motor controlled spectrometer to select sections of the spectrum with a bandwidth of 12 nm. The entire setup had an instrumental response function (IRF) of 120−180 fs. Pump and probe beam were focused weakly under an angle of 10° with magic angle polarization on a 1 mm cuvette with a spot diameter of 600 and 300 $\mu$m, respectively. In the spectral region of the fundamental wavelength (780 nm ± 15 nm) the experimental error is higher due to two effects: (I) The straylight of the pump beam cannot be eliminated by band-pass filters. This effect can partly be corrected for by subtraction of the straylight at negative delay. (II) Whitelight generation is a highly nonlinear process. This decreases the relative contribution of small pulses following the main probe pulse with a delay of some nanoseconds drastically in all spectral regions except for the generation wavelength.

Transient absorption spectra of [Mg]- and [Zn]-BChl were performed at 100 ps and 1 ns after excitation at 780 nm by four different scan cycles (450−550 nm, 550−650 nm, 650−750 nm, and 750−900 nm, respectively, to avoid sample degradation due to prolonged exposure to excitation light (see below). The higher stability of [Zn]-BChl allowed the measurement of transient absorption spectra in the examined spectral range (450−900 nm) in 20 nm steps with the same sample in one measurement cycle.

**Time-Resolved Fluorescence.** Time-correlated single-photon-counting (TCSPC) results were obtained with an experimental setup described elsewhere.[7] The IRF fwhm for those measurements was 35−40 ps.

Femtosecond time-resolved fluorescence was measured with the upconversion technique as described in refs 7 and 28 and is briefly described in the following. The laser source was a Ti:sapphire oscillator (Coherent Mira Basic), pumped by 8 W of the output of an $Ar^+$ laser (Coherent Innova 425). The laser delivered at least 450 mW of average power at the desired excitation wavelengths. Pulse repetition rate was 76 MHz. After compression with a four-prism (SF10) chirp compensation, we got pulse widths below 100 fs. The laser beam was split in two parts with equal power, one focusing onto the sample (pulse energy 0.7 nJ, spot diameter 50 $\mu$m), the other one (gate beam) passing a stepping motor driven delay stage (resolution 16.7 fs, range 1.3 ns). The latter was combined with the fluorescence

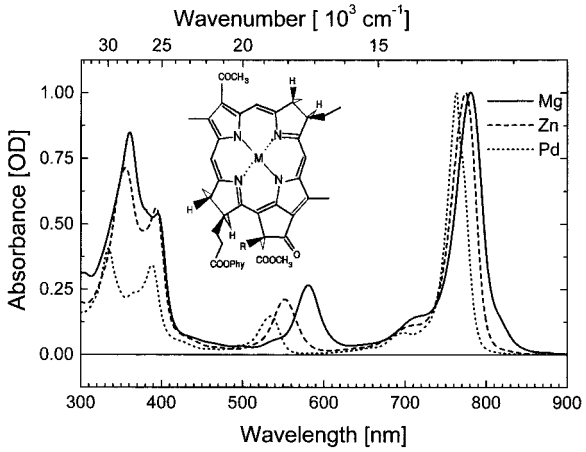


**Figure 1.** Absorption spectra of metal-substituted BChl in toluene at 290 K, normalized to identical $Q_y$ absorption maximum: [Mg]-BChl (—), [Zn]-BChl (- - -), and [Pd]-BChl (···). The inset shows the structural formula of the complexes (M = Mg, Zn, Pd; R = H, OH).

from the sample in a $\beta$-barium borate (BBO) crystal (thickness 1 mm) under an angle of 11°, thus allowing noncritical type I phase matching. The geometry was chosen to upconvert fluorescence being polarized parallel to the excitation. The sample cell was rotating with up to 3000 rpm to reduce sample degradation by distributing the excitation energy over a larger sample volume. The intensity of sum frequency light is detected with a photomultiplier (Hamamatsu R4220P) after passing a double monochromator (Jobin Yvon HD20). The sum frequency photons were separated from the remaining background photons by counting them synchronously to the phase of light choppers in the excitation and gate pathways. To reduce the influence of long-term drifts of the laser and degradation of the samples upon the decay curves, we collected up to 32 individual time traces and altered the direction of acquisition after each run.

The IRF was taken before each fluorescence measurement using scattered light from the sample. The alignment was not changed except for adjusting the phase-matching angle of the crystal and the detection wavelength in order to achieve an optimized signal-to-noise ratio. The full width at half-maximum (fwhm) of the IRF was about 140 fs.

**Fitting Procedure.** Time constants were extracted from the experimental transient absorption and fluorescence data by fitting a convolution of the experimental IRF and exponential decay functions to the data using the Levenberg−Marquardt method. This deconvolution method the resolved lifetimes down to a quarter of the IRF fwhm. The IRF of the absorption measurements was a free Gaussian parameter. The quality of fit was judged by observing the residuals and values of the reduced $\chi_\nu^2$.

## Results and Discussion

**Steady-State Absorption and Fluorescence.** The ground-state absorption spectra of [Mg]-, [Zn]-, and [Pd]-BChl dissolved in toluene are shown in Figure 1. All spectra exhibit the expected four electronic transitions in the UV to NIR region (the $B_y$, $B_x$, $Q_x$, and $Q_y$ transitions in order of decreasing energy). The respective maxima are located at 361, 395, 581, and 781 nm for [Mg]-BChl, at 355, 393, 555, and 773 nm for [Zn]-BChl, and at 334, 388, 535, and 762 nm for [Pd]-BChl. The corresponding $13^2$-hydroxy derivatives exhibit identical absorption properties except for a systematical blue shift of the $Q_x$ band of ∼5 nm. The absorption maxima compare well to literature data for these complexes dissolved in diethyl ether.[19]

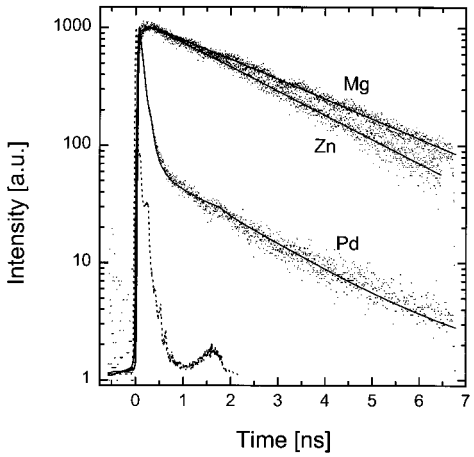


**Figure 2.** Spontaneous fluorescence decay of [Mg]-BChl ($\lambda_{em}$ = 860 nm), [Zn]-BChl ($\lambda_{em}$ = 830 nm), and [Pd]-BChl ($\lambda_{em}$ = 780 nm) in toluene at 290 K measured by TCSPC.

[Mg]- and [Zn]-BChl fluoresce 20 nm shifted to the $Q_y$ absorption at 800 and 790 nm, whereas [Pd]-BChl shows no fluorescence under these conditions.

The lowest excited states of all examined [M]-BChl are located in the near-infrared, exhibiting a singlet−triplet splitting of about 4550 $cm^{-1}$,[17,19,53] somewhat smaller than that of chlorins and porphyrins. Thus, increased intersystem crossing rates from $S_1$ to $T_1$ can be expected. The low lying $S_1$ states in [M]-BChl provide that empty (d,d) states of most transition metals (including $Pd^{2+}$ [42]) are higher and metal-induced spin−orbit coupling effects on the $S_1$ ($\pi-\pi^*$) excitation can be studied without interference of transient populations of metal-centered states.

**Time-resolved fluorescence** of [Mg]-, [Zn]-, and [Pd]-BChl probed at 860, 830, and 780 nm, respectively, is depicted in Figure 2. The detection wavelength is kept at the red wing of the steady-state fluorescence maxima (788, 782, and 764 nm, respectively[19]) to avoid stray light. All decay traces can be fitted sufficiently with a single-exponential component. The $S_1$ decay lifetimes are 2.6 ns, 2.1 ns, and 65 ps for [Mg]-BChl, [Zn]-BChl, and [Pd]-BChl, respectively. A negligible contribution (<5% amplitude) of a 2 ns component is observed in the [Pd]-BChl fluorescence decay probably due to a minor amount (<1%) of BPhe or BChl impurities. The depopulation of $S_1$ in [Mg]-BChl is in agreement with previously reported values for the singlet lifetime, 2.2−3.0 ns[54−56] depending on the solvent used. The value for [Zn]-BChl is close to the decay times measured for various zinc porphyrins (2−3 ns).[42,57,58]

All [M]-BChl were tested for the existence of faster decay components by fluorescence upconversion with a 100 fs time resolution. Examples of time traces are given in Figure 3. These measurements did not reveal any decay components (including vibrational relaxation processes or dynamic Stoke shifts) faster than the TCSPC-detected decay. Due to the high power, high repetitive excitation of the upconversion laser system, a significant decrease of the signal was observed for [Mg]- and [Zn]-BChl within the first hour of data collection. Obviously, these conditions lead to radiation damage in these complexes, whereas no such effect is observed for [Pd]-BChl. Concomitant with the sample degradation an additional 1 ps decay component with gradually increasing amplitude appears for [Zn]-BChl (Figure 3a). For [Mg]-BChl the high power, high repetitive excitation leads to the appearance of several short-living fluorescence components. This behavior is discussed in more detail below in combination with the corresponding transient absorption data.

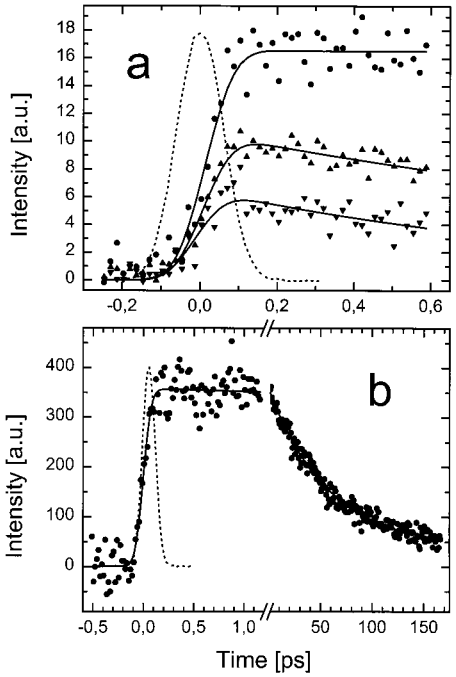


**Figure 3.** Fluorescence upconversion measurements and IRF (···) of (a) [Zn]-BChl in toluene at 290 K: development of the signal within the first 15 min (●), the next 30 min (▲) and the last 15 min (▼) of 1 h our observation and (b) [Pd]-BChl in toluene at 290 K.

**Transient Absorption.** *(a) BChl.* Transient absorption experiments performed with this Mg complex at 50 Hz did not lead to a detectable sample degradation, whereas already 500 Hz experiments showed a destruction of [Mg]-BChl concomitant with the appearance of several new components with fast decay times (<10 ps). To avoid any sample degradation, we thus performed the experiments on [Mg]-BChl at 50 Hz repetition rate.

Excitation at 780 nm leads to an instantaneous bleaching of the ground-state absorption bands located at 581 and 781 nm (Figure 4a). Simultaneously the appearance of a broad transient absorption ranging from the blue edge of our spectral window into the $Q_y$ region is observed. The negative transient absorption around 800 nm is ∼300 $cm^{-1}$ red-shifted with respect to the ground-state absorption and actually is composed of ground-state bleaching and stimulated emission. The sharp shape of the transient spectrum around the $Q_y$ transition in comparison with the ground-state absorption is probably caused by the high error due to white-light probing (see Experimental Section). The transient absorption spectrum does not change within the first 100 ps. Typical decay traces at 640 and 780 nm depicted in Figure 5a show that there is a component decaying with a lifetime larger than our maximum delay time (1.5 ns), in agreement with the 2.6 ns $S_1$ decay time measured in time-resolved fluorescence. Thus, the transient absorption spectrum of Figure 4a represents solely the absorption changes due to formation of $S_1$ in BChl (i.e., it is a superposition of ground-state bleaching, stimulated emission, and $S_1$ absorption). The underlying broad and unstructured transient $S_1$ absorption ranging from 450 to 750 nm exhibits a weak maximum around 660 nm. The broad steady-state absorption spectrum in the Soret region around the $B_y$ transition at 361 nm ($B_y-Q_y$ energy difference: 14 900 $cm^{-1}$, 671 nm) indicates the contribution of the $Q_y \rightarrow B_y$ transition to the observed positive $S_1$ absorption. All features of the transient absorption spectrum (ground-state bleaching, stimulated emission, and transient absorption) vary

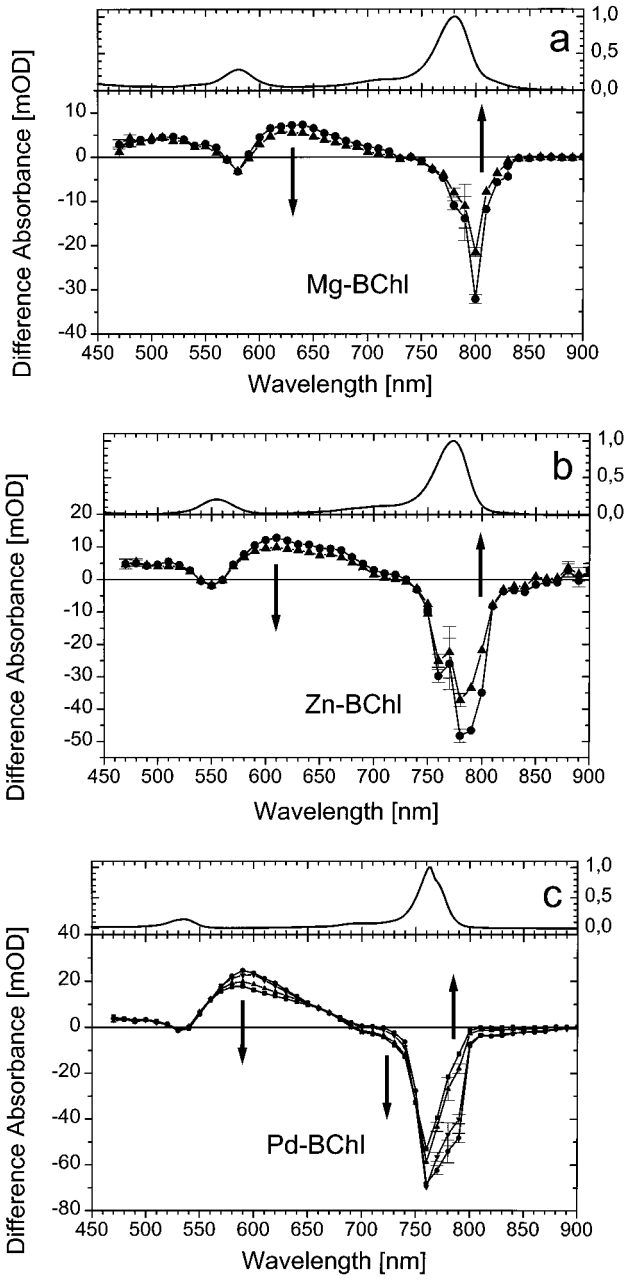


**Figure 4.** Ground-state absorbance (top) and transient absorption spectra of (a) [Mg]-BChl at 100 ps (●) and 1 ns (▲) after excitation at 780 nm (b) [Zn]-BChl at 100 ps (●) and 1 ns (▲) after excitation at 780 nm, and (c) [Pd]-BChl at 1 ps (●), 10 ps (▼), 100 ps (▲), and 1.5 ns (■) after excitation at 780 nm; arrows indicate the temporal evolution of the spectra

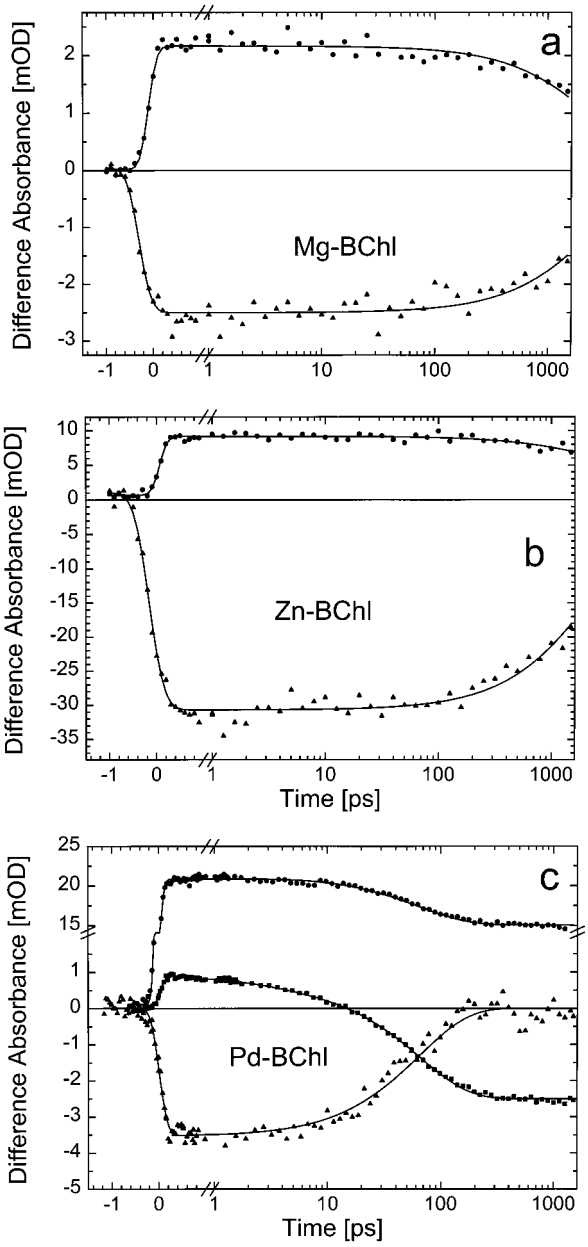


**Figure 5.** Transient absorption decay of (a) [Mg]-BChl probed at 640 nm (●) and 780 nm (▲) with 50 Hz excitation repetition rates, (b) [Zn]-BChl probed at 640 nm (●) and 780 nm (▲) with 50 Hz excitation repetition rates, and (c) [Pd]-BChl probed at 600 nm (●), 710 nm (■), and 820 nm (▲) with 500 Hz excitation repetition rate (solid lines: least-squares fit of the experimental data).

with the same time constant over the entire examined wavelength range.

The transient absorption and fluorescence data at low excitation power and low repetition rate contrast the results of high repetitive femtosecond pump−probe experiments done by Savikhin and Struve.[59] They found a multiexponential time dependency of the ground-state recovery and stimulated emission of [Mg]-BChl *a* in 1-propanol upon excitation of the $Q_y$ band, and these observations were assigned to vibrational cooling and dielectric relaxation in the spectral range around the $Q_y$ transient. Since we get a similar multiexponential decay only at higher repetition rate concomitant with sample degradation, we suggest that the occurrence of decay components faster than about 2−3 ns upon $Q_y$ excitation of [Mg]-BChl actually is related to secondary effects after multiple excitation. This assignment is corroborated by the reported millisecond triplet lifetime of [Mg]-BChl[57] enabling multiphoton absorption processes at higher rep rates.

*(b) [Zn]-BChl.* Photochemically, [Zn]-BChl is more stable than the Mg complex, but it was still necessary to keep the repetition rate at 50 Hz to avoid the multiexponential behavior resulting from sample degradation. The transient absorption spectrum recorded 100 ps after excitation (Figure 4b) is similar to the one obtained for [Mg]-BChl. Again a broad transient absorption appears ranging from the UV to the $Q_y$ region with a notch around the $Q_x$ absorption due to $Q_x$ bleaching and a slight maximum around 660 nm ($B_y-Q_y$ energy difference: 15 230 $cm^{-1}$, 657 nm). Around 773 nm the ground-state bleaching is observed and 20 nm red-shifted stimulated emission appears. Typical decay traces at 640 and 780 nm are shown in Figure 5b. Each decay can be fitted monoexponentially with

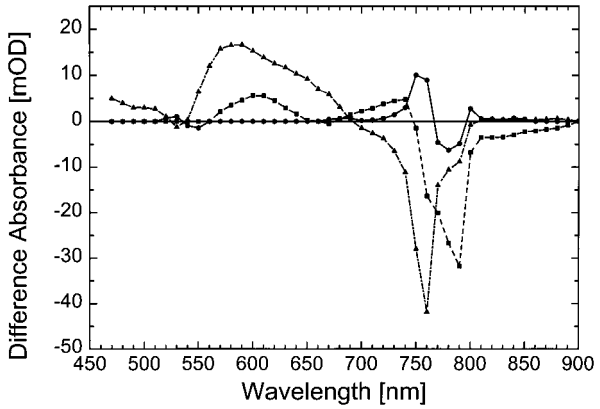


**Figure 6.** Decay-associated spectra (wavelength-dependent amplitudes) of the transient absorption of [Pd]-BChl of the 3 ps (●) and 65 ps (■) component and the remaining offset at 1.5 ns (▲) after excitation

decay times of 2.1 ns, in agreement with the $S_1$ lifetime detected in fluorescence. Using this information, it is possible to approximate the pure transient triplet absorption spectrum of [Zn]-BChl showing a spectral characteristic similar to transient triplet absorption of BChl.[60]

*(c) [Pd]-BChl.* The most stable complex under investigation, [Pd]-BChl, could be examined at an excitation repetition rate of 500 Hz, providing high-resolution transient absorption data. Figure 4c displays transient absorption spectra of [Pd]-BChl at various delay times after excitation at 780 nm. At 1 ps delay the transient absorption displays the typical broad excited-state absorption with little structure and a weak maximum around 590 nm ($B_y-Q_y$ energy difference: 16 800 $cm^{-1}$, 595 nm) superimposed by the $Q_x$ ground-state bleaching around 535 nm, the $Q_y$ bleaching around 762 nm, and the stimulated emission around 790 nm. In contrast to [Mg]- and [Zn]-BChl the transient absorption spectrum of [Pd]-BChl shows some dynamics within the first 100 ps, and decay traces recorded at different wavelengths can be summarized as follows. Between 460 and 510 nm almost no temporal evolution is observed during the first 1.5 ns. The transient absorption signal around the $Q_x$ transition at 535 nm shows a minor fast (∼3 ps) decay component. Between 560 and 740 nm a more pronounced decrease of the signal proceeds with 65 ps, but around 670 nm there is almost no temporal evolution of the transient absorption during the complete observation time of ∼1.5 ns. The signal around 780 nm is biexponential (lifetimes of 65 and 3 ps), and between 800 and 900 nm it is dominated again by a mono-exponential 65 ps decay of simulated emission (in accordance with upconversion and TCSPC measurements). Typical decay traces at 600, 710, and 820 nm are depicted in Figure 5c.

To distinguish between the different processes connected with the individual kinetics, we constructed decay-associated spectra (DAS) for [Pd]-BChl, i.e., the preexponential amplitudes of each observed time constant as a function of detection wavelength (Figure 6). According to the DAS, the assignment of the dominating 65 ps component to $S_1$ depopulation is mainly consistent with the transient absorption observed in [Mg]-BChl or [Zn]-BChl with a maximum for the $Q_y$ to $B_y$ transition located around 600 nm. The most prominent deviation occurs above 650 nm, where we observed a well-separated positive absorption which might be due to an additional transient. No ground-state recovery is detectable in the $Q_x$ absorption (535 nm) within the first 1.5 ns, indicating a very high triplet yield.[18] The signal at wavelengths > 780 nm is characterized by pure stimulated emission exhibiting a shoulder into the NIR. The 1.5 ns spectrum reflects the transient triplet absorption spectrum with the remaining ground-state bleaching and is similar to the corresponding features in [Mg]- and [Zn]-BChl.

Finally, we report on one specific feature of [Pd]-BChl depicted in Figure 6. Within our time resolution of 120 fs there is a sigmoidal shift in the regions of the ground-state absorption bands which decays with 3 ps. This feature adds a small ampludude (<10%) to the overall recovery dynamics of the ground-state absorption bands. This 3 ps decay time is not observed in fluorescence measurements. Experiments are in progress that investigate whether this 3 ps component is related to specific features of a small fraction of [Pd]-BChl aggregates.

**Elementary Photophysical Properties of [Mg]-, [Zn]-, and [Pd]-BChl.** The above results of the time-resolved experiments on [Mg]-, [Zn]-, and [Pd]-BChl can be explained by a simple three-level model including the $S_0$ ground state, the excited singlet state $S_1$, and the excited triplet state $T_1$ of the tetrapyrrole $\pi$-system. The lifetime of the $S_1$ state is given by

$$\tau_{S_1} = \frac{1}{k_F + k_{IC} + k_{ISC}} \quad (1)$$

with $k_F$ as the fluorescence rate, $k_{IC}$ as the internal conversion (IC) rate to the ground state, and $k_{ISC}$ as the intersystem crossing (ISC) rate to the $T_1$ state.

The internal conversion rate for [Mg]-BChl of $k_{IC} = 1.7 \times 10^7\ s^{-1}$ reported previously by Teuchner et al.[56] is assumed to be identical for all [M]-BChls examined. This assumption is justified since $k_{IC}$ is determined by the "energy gap law" in the limit of weak electronical coupling,[61,62] i.e., it is limited by the energy of the fluorescence which is almost identical for the three complexes. The fluorescence decay rate $k_F$ can be estimated by the Strickler−Berg relation[63]

$$k_F = 8\pi c n^2 \langle \tilde{\nu}^{-3} \rangle^{-1} \int \frac{\epsilon(\tilde{\nu})}{\tilde{\nu}} d\tilde{\nu}$$

$$\langle \tilde{\nu}^{-3} \rangle := \int F(\tilde{\nu}) \tilde{\nu}^{-3}\, d\tilde{\nu} \quad (2)$$

from the normalized fluorescence spectrum $F$ and the extinction coefficient $\epsilon(\tilde{\nu})$ reported in ref 19 for the $Q_y$ absorption band ($c$ is the speed of light, $n$ the refraction index of the solvent, and $\tilde{\nu}$ the wavenumber), yielding intrinsic lifetimes $\tau_0 = 1/k_F$ of 14, 19, and 13 ns for the $Mg^{2+}$-, $Zn^{2+}$-, and $Pd^{2+}$-centered BChl, which is consistent with literature data for [Mg]-BChl.[54−56] Because of the missing fluorescence spectrum observed in [Pd]-BChl, we used the approximation of $\langle \tilde{\nu}^{-3} \rangle := \tilde{\nu}_{abs}^{-3}$ with the energetical position of the $Q_y$ transition $\nu_{abs}$.

Both, $k_F$ and $k_{IC}$ are far from dominating the actual $S_1$ lifetime, showing that the main dacay channel is ISC to the lowest triplet state $T_1$. The triplet yield $\Phi_{ISC}$ for [Mg]-BChl of 76.7% is somewhat higher than some literature data[54,64] but is in accordance with a more recent publication.[56] It is also corroborated by the relative $Q_x$ ground-state recovery due to triplet-state formation of the pigments under investigation, which is a measure for $\Phi_{ISC}$. For [Zn]-BChl ($\Phi_{ISC} = 85.4\%$) similar quantum yields for ISC are reported for Zn porphyrins.[57] The extremely high value of $\Phi_{ISC} > 99\%$ for [Pd]-BChl is due to the heavy atom effect of Pd and is consistent with measurements at Pd porphyrins.[65] The corresponding data for the examined complexes are summarized in Table 1.

In agreement with the singlet−triplet splitting of about 4550 $cm^{-1}$ for the [M]-BChls,[17,19,53] a strong phosphorescence can be detected for [Pd]-BChl[18] in the absence of $O_2$ peaking at 1170 nm. In the presence of $O_2$ the phosphorescence is completely quenched and the typical $^1O_2$ emission at 1230 nm

**TABLE 1: Photophysical Properties of [M]-BChls in Toluene**

| [M]-BChl M = | $\tau_{S_1}$ | $k_F$ [$10^7$ $s^{-1}$] | $k_{IC}$ [$10^7$ $s^{-1}$] | $k_{ISC}$ [$10^8$ $s^{-1}$] | $\Phi_F = k_F\tau_{S_1}^{-1}$ | $\Phi_{IC} = k_{IC}\tau_{S_1}^{-1}$ | $\Phi_{ISC} = k_{ISC}\tau_{S_1}^{-1}$ |
|---|---|---|---|---|---|---|---|
| Mg | 2.6 ns | 7.2 | 1.7 | 3.0 | 18.9% | 4.4% | 76.7% |
| Zn | 2.1 ns | 5.3 | 1.7 | 4.1 | 11.0% | 3.6% | 85.4% |
| Pd | 65 ps | 6.9 | 1.7 | 153 | 0.5% | 0.1% | 99.4% |

is detected, whereas no significant phosphorescence quenching by $O_2$ was detectable for [Zn]-BChl.[18] This behavior clearly demonstrates not only that excitation of [Pd]-BChl results in almost complete formation of its triplet state but also that this triplet state transfers its energy efficiently onto oxygen to produce the highly toxic singlet $^1O_2$. This reaction sequence might be utilized for directed photosensitized destruction of tumor tissue. Excellent photodynamic behavior of a [Pd]-BChl derivative has been observed.[14]

## Conclusions

We have provided the elementary photophysical properties of BChl *a* and its Zn and Pd derivatives resulting upon excitation into the redmost absorption of these complexes. In each case instantaneous ground-state absorption bleaching is superimposed by broad, but weak $S_1$ absorption in the complete visible range with minor structure. The $S_1$ state decays with a lifetime of 2−2.6 ns in [Mg]- and [Zn]- BChl and with 65 ps in [Pd]-BChl with a main deactivation pathway into the triplet state of the tetrapyrrole $\pi$-system. The spectral characteristics of the $T_1$ state are similar for all examined complexes and mainly resemble those of the corresponding $S_1$ states, but with smaller absorption cross sections for the excitation into higher triplet states. An increased intersystem crossing rate for [Pd]-BChl yielding almost 100% $T_1$ formation is attributed to the heavy atom effect of the open shell $Pd^{2+}$ central ion. The $T_1$ state of [Pd]-BChl is almost completely quenched by the presence of oxygen, forming $^1O_2$, supporting its potential as an excellent sensitizer for photodynamic therapy.

**Acknowledgment.** We thank M. A. J. Rodgers, Yellow Springs, for carrying out preliminary luminescence experiments on several of our [M]-BChl. We thank D. Leupold, Berlin, and A. Scherz, Rehovot, for communicating independent spectroscopic results on transmetalated bacteriochlorophyll prior to publication. We gratefully acknowledge the financial support by the Deutsche Forschungsgemeinschaft SFB 143, SFB 533.

## References and Notes

(1) Scheer, H., Ed. *Chlorphylls;* CRC Press: Boca Raton, FL, 1991.
(2) Vos, M. H.; Breton, J.; Martin, J.-L. *J. Phys. Chem. B* **1997**, *101*, 9820−9832.
(3) Jonas, D. M.; Lang, M. J.; Nagasawa, Y.; Joo, T.; Fleming, G. R. *J. Phys. Chem.* **1996**, *100*, 12660−12673.
(4) Stanley, R. J.; King, B.; Boxer, S. G. *J. Phys. Chem.* **1996**, *100*, 12052−12059.
(5) Haran, G.; Wynne, K.; Moser, C. C.; Dutton, P. L.; Hochstrasser, R. M. *J. Phys. Chem.* **1996**, *100*, 5562−5569.
(6) Lin, S.; Taguchi, A. K. W.; Woodbury, N. W. *J. Phys. Chem.* **1996**, *100*, 17067−17078.
(7) Hartwich, G.; Lossau, H.; Ogrodnik, A.; Michel-Beyerle, M. E. In *The Reaction Center of Photosynthetic Bacteria;* Michel-Beyerle, M. E., Ed.; Springer: Berlin, 1996; pp 199−215.
(8) Kirmaier, C.; Holten, D. *Photosynth. Res.* **1987**, *13*, 225−260.
(9) Kirmaier, C.; Holton, D. In *The Photosynthetic Reaction Center;* Deisenhofer, J., Norris, J. R., Eds.; Academic Press: San Diego, 1993; Vol. II, pp 49−70.
(10) Zinth, W.; Kaiser, W. In *The Photosynthetic Reaction Center;* Deisenhofer, J., Norris, J. R., Eds.; Academic Press: San Diego, 1993; Vol. II, 71−88.
(11) Spikes, R. K.; Bommer, J. C. In *Chlorophylls;* Scheer, H., Ed.; CRC Press; Boca Raton, FL, 1991; pp 1181−1204.
(12) Pandey, R. K.; Bellnier, D. A.; Smith, K. M.; Dougherty, T. J. *Photochem. Photobiol.* **1991**, *53*, 65−72.
(13) Pandey, R. K.; Shiau, F. Y.; Sumlin, A. B.; Dougherty, T. J. *Bioorg. Med. Chem. Lett.* **1994**, *4*, 1263−1267.
(14) Moser, J. G.; Suchomski, R.; Danielowski, T.; Wagner, B.; Scheer, H.; Hartwich, G. *SPIE Proceedings of the 5th Biennal Meeting IPA,* Amelia Island FA, 1995; 2371, pp 178−186.
(15) Rosenbach-Belkin, V.; Chen, L.; Fiodor, L.; Tregub, I.; Pavlotsky, F.; Brumfeld, V.; Salomon, Y.; Scherz, A. *Photochem. Photobiol.* **1996**, *64*, 174−181.
(16) Boyle, R. W.; Dolphin, D. *Photochem. Photobiol.* **1996**, *64*, 469−485.
(17) Moser, H. J. *Photodynamic Tumor Therapy*; Warwood, 1998.
(18) Rodgers, M. A. J.; Hartwich, G.; Scheer, H. Unpublished. A sceening of several [M]-BChl was done in collaboration with M. A. J. Rodgers and indicated particularly triplet and $^1O_2$ quantum yields for [Pd]-BChl.
(19) Hartwich, G.; Fiedor, L.; Simonin, I.; Cmiel, E.; Schäfer, W.; Noy, D.; Scherz, A.; Scheer, H. *J. Am. Chem. Soc.* **1998**, *120*, 3675−3683.
(20) Losev, A. P.; Knyukshto, V. N.; Kochubeeva, N. D.; Solovev, K. N. *Opt. Spectrosc.* **1991**, *97*, 97−101.
(21) Donohoe, R. J.; Frank, H. A.; Bocian, D. F. *Photochem. Photobiol.* **1988**, *48*, 531−537.
(22) Geskes, C.; Hartwich, G.; Scheer, H.; Mäntele, W.; Heintze, W. J. *J. Am. Chem. Soc.* **1995**, *117*, 7776−7783.
(23) Hartwich, G.; Geskes, C.; Scheer, H.; Heintze, J.; Mäntele, W. *J. Am. Chem. Soc.* **1995**, *117*, 7784−7790.
(24) Noy, D.; Fiedor, L.; Hartwich, G.; Scheer, H.; Scherz, A. *J. Am. Chem. Soc.* **1998**, *120*, 3684−3693.
(25) Renner, M. W.; Zhang, Y.; Noy, D.; Scherz, A.; Smith, K. M.; Fajer, J. In *Reaction Centers of Photosynthetic Bacteria;* Michel-Beyerle, M. E., Ed.; Springer-Verlag: Berlin, 1996; pp 369−380.
(26) Hartwich, G.; Friese, M.; Scheer, H.; Ogrodnik, A.; Michel-Beyerle, M. E. *Chem. Phys.* **1995**, *197*, 423−434.
(27) Scheer, H.; Hartwich, G. In *Anoxygenic Photosynthetic Bacteria;* Blankenship, R. E., Madigan, M. T., Bauer, C. E., Eds.; Kluwer: Dordrecht, 1995; pp 649−664.
(28) Häberle, T.; Lossau, H.; Friese, M.; Hartwich, G.; Ogrodnik, A.; Scheer, H.; Michel-Beyerle, M. E. In *The Reaction Center of Photosynthetic Bacteria;* Michel-Beyerle, M. E., Ed.; Springer: Berlin, 1996; pp 239−254.
(29) Chen, L. X.; Wang, Z. Y.; Hartwich, G.; Katheder, I.; Scheer, H.; Scherz, A.; Montano, P. A.; Norris, J. R. *Chem. Phys. Lett.* **1995**, *234*, 437−444.
(30) Frank, H.; Chynwat, V.; Hartwich, G.; Meyer, M.; Katheder, I.; Scheer, H. *Photosyn. Res.* **1993**, *37*, 193−203.
(31) Frank, H.; Chynwat, V.; Posteraro, A.; Hartwich, G.; Simonin, I.; Scheer, H. *Photosyn. Res.* **1996**, *64*, 823−831.
(32) Hartwich, G.; Scheer, H.; Aust, V.; Angerhofer, A. *Biochim. Biophys. Acta* **1995**, *1230*, 97−113.
(33) Bixon, M.; Jortner, J.; Michel-Beyerle, M. E. *Chem. Phys.* **1995**, *197*, 389−404.
(34) Hyninnen, P. H. In *Chlorophylls;* Scheer, H., Ed.; CRC Press: Boca Raton, FL, 1991; pp 145−209.
(35) Watanabe, T.; Kobayashi, M. In *Chlorophylls;* Scheer, H. Ed.; CRC Press: Boca Raton, FL, 1991; pp 282−316.
(36) Barkigia, K. M.; Chantranupong, L.; Fajer, J.; Smith, K. M. *J. Am. Chem. Soc.* **1988**, *110*, 7566−7567.
(37) Buchler, J. W. In *Porphyrins and Metalloporphyrins;* Smith, K. M., Ed.; Elsevier Publishing: New York, 1975; pp 157−232.
(38) Gouterman, M. *J. Chem. Phys.* **1959**, *30*, 1139−1161.
(39) Gouterman, M. *J. Mol. Spectrosc.* **1963**, *11*, 108−127.
(40) Hanson, L. K. In *Chlorophylls;* Scheer, H., Ed.; CRC Press: Boca Raton, FL 1991; pp 993−1041.
(41) Scherz, A.; Rosenbach-Belkin, V.; Michalski, T. J.; Worchester, D. L. In *Chlorophylls*; Scheer, H., Ed.; CRC Press: Boca Raton, FL, 1991; pp 237−268.
(42) Kobayashi, T.; Straub, K. D.; Rentzepis, P. M. *Photochem. Photobiol.* **1979**, *29*, 925−931.
(43) Rodriguez, J.; Kirmaier, C.; Holten, D. *J. Am. Chem. Soc.* **1989**, *111*, 6500−6506.
(44) Straub, K. D.; Rentzepis, P. M.; Huppert, D. *J. Photochem.* **1981**, *17*, 419−425.
(45) Rodriguez, J.; Holten, D. *J. Chem. Phys.* **1989**, *91*, 3525−3531.
(46) Rodriguez, J.; Holten, D. *J. Chem. Phys.* **1990**, *92*, 5944−5950.
(47) Stiel, H.; Teuchner, K.; Hild, M.; Freyer, W.; Leupold, D.; Simonin, I.; Hartwich, G.; Scheer, H.; Noy, D.; Brumfeld, V.; Scherz, A. To be submitted to *J. Am. Chem. Soc*.
(48) Scheer, H.; Struck, A. In *The Photosynthetic Reaction Center*; Norris, J. R., Deisenhofer, J., Eds.; Academic Press: New York, 1993; pp 157−192.

(49) Struck, A.; Cmiel, E.; Katheder, I.; Schäfer, W.; Scheer, H. *Biochim. Biophys. Acta* **1992**, *1101*, 321−328.
(50) Omata, T.; Murata, N. *Plant Cell Physiol.* **1983**, *24*, 1093−1100.
(51) Schaber, P. M.; Hunt, J. E.; Fries, R.; Katz, J. J. *J. Chromatogr.* **1984**, *316*, 25−41.
(52) Rosenbach-Belkin, V. Ph.D. Thesis, The Weizmann Institut of Science, Rehovot, Israel, 1988.
(53) Takiff, L.; Boxer, S. G. *Biochim. Biophys. Acta* **1988**, *932*, 325−334.
(54) Connolly, J. S.; Samuel, E. B.; Janzen, A. F. *Photochem. Photobiol.* **1982**, *36*, 565−574.
(55) Becker, M.; Nagarajan, V.; Parson, W. W. *J. Am. Chem. Soc.* **1991**, *113*, 6840−6848.
(56) Teuchner, K.; Stiel, H.; Leupold, D.; Katheder, I.; Scheer, H. *J. Lumin.* **1994**, *60*−*61*, 520−522.
(57) Harriman, A. *J. Chem. Soc. Faraday Trans. 1* **1980**, *76*, 1978−1985.
(58) Ohno, O.; Kaizu, Y.; Kobayashi, H. *J. Chem. Phys.* **1985**, *82*, 1779−1787.
(59) Savikhin, S.; Struve, W. S. *Biophys. J.* **1994**, *67*, 2002−2007.
(60) Shuvalov, V. A.; Parson, W. W. *Biochim. Biophys. Acta* **1981**, *638*, 50−59.
(61) Englman, R.; Jortner, J. *Mol. Phys.* **1970**, *18*, 145−164.
(62) Fischer, S. F. *J. Chem. Phys.* **1970**, *53*, 3195−3207.
(63) Strickler, S. J.; Berg, R. A. *J. Chem. Phys.* **1962**, *37*, 814−822.
(64) Gurinovich, G. P.; Losev, A. P.; Segun, E. I. *J. Appl. Spectrosc. (USSR)* **1976**, *26*, 740−744.
(65) Magde, D.; Gouterman, M. *Chem. Phys. Lett.* **1974**, *29*, 183−187.